A Novel Bayesian Semi-parametric Model for Learning Heritable Imaging Traits

Yize Zhao[1], Xiwen Zhao[1], Mansu Kim[2], Jingxuan Bao[2], and Li Shen[2(✉)]

[1] Department of Biostatistics, Yale University School of Public Health,
New Haven, NJ, USA
yize.zhao@yale.edu
[2] Department of Biostatistics, Epidemiology, and Informatics,
University of Pennsylvania Perelman School of Medicine, Philadelphia, PA, USA
li.shen@pennmedicine.upenn.edu

Abstract. Heritability analysis is an important research topic in brain imaging genetics. Its primary motivation is to identify highly heritable imaging quantitative traits (QTs) for subsequent in-depth imaging genetic analyses. Most existing studies perform heritability analyses on regional imaging QTs using predefined brain parcellation schemes such as the AAL atlas. However, the power to dissect genetic underpinnings under QTs defined in such an unsupervised fashion is largely deteriorate with inner partition noise and signal dilution. To bridge the gap, we propose a new semi-parametric Bayesian heritability estimation model to construct highly heritable imaging QTs. Our method leverages the aggregate of genetic signals to imaging QT construction by developing a new brain parcellation driven by voxel-level heritability. To ensure biological plausibility and clinical interpretability of the resulting brain heritability parcellations, hierarchical sparsity and smoothness, coupled with structural connectivity of the brain, are properly imposed on genetic effects to induce spatial contiguity of heritable imaging QTs. Using the ADNI imaging genetic data, we demonstrate the strength of our proposed method, in comparison with the standard GCTA method, in identifying highly heritable and biologically meaningful new imaging QTs.

Keywords: Imaging genetics · Heritability estimation · Bayesian semi-parametric modeling

1 Introduction

Brain imaging genetics is an emerging and rapidly growing data science field that arises with the recent advances in acquiring multimodal neuroimaging data and high throughput genotyping and sequencing data [9,14,16,23]. To characterize

genetic contributions on heritable neuroimaging quantitative traits (QTs), we are able to gain new insights into the pathobiological mechanism from genetics to brain structure and function, and their impact on behaviors and diseases.

The concept of heritability [19] has thus emerged under imaging genetics paradigm to describe the proportion of the total imaging phenotypic variance that is explained by the aggregated genetic effect captured by pedigree information [17] or all the single nucleotide polymorphisms (SNPs) on a genotyping array [24]. Under existing heritability studies, atlas-based brain parcellations like automated anatomical labeling (AAL) [18] are routinely used to define imaging traits based on certain imaging modality. However, within each region of interest (ROI) defined under such an unsupervised brain parcellation, some areas may be impacted marginally by SNPs, leading to a dilution of power to dissect genetic contribution. Thus, there is an urgent need to construct a heritability map at voxel level to accurately provide cartography for the truly heritable brain areas.

It is a challenging task to accurately construct a biological interpretable heritability map over whole brain voxel-wise neuroimaging measurements. Most of the existing heritability modeling [5,22], including the widely used genome-wide complex trait analysis (GCTA) [22], can only handle univariate phenotype without an efficient way to accommodate the phenotypic correlation. A few recent attempts [6,10,25] start to explore heritability analysis for multivariate or large-scale phenotypes especially given the highly correlated collections from neuroimaging data. Those methods, though providing promising results under their applications, are either unable to handle high-dimensional phenotypes like the voxel-wise traits due to a direct inverse of the phenotypic covariance matrix, or fail to incorporate biologically plausible assumptions like the smoothness over brain topology for the heritability estimates.

In this paper, we propose a new Bayesian joint voxel-wise heritability analysis to construct highly heritable imaging QTs based on the estimated heritability map. From the analytical perspective, this requires an efficient and meaningful variance component selection under high dimensional imaging responses. Despite there is a broad literature on Bayesian sparsity and shrinkage, almost none of them deals with the selection and estimation on the variance components. Under neuroimaging studies with unique spatial correlation across voxels and structural/functional interactions among ROIs, we also need to properly consider the underlying biological information, which otherwise will cause a power loss in heritable traits detection and implausible interpretation.

To address all the above limitations and challenges, we propose a new semi-parametric Bayesian heritability estimation model, and apply it to the imaging genetic data from the Alzheimer's Disease Neuroimaging Initiative (ADNI) [12, 15,20] to construct highly heritable and biologically meaningful imaging QTs. Our major contributions are summarized as follows:

– We create a brain heritability map under a novel Bayesian integrative heritability analysis for high dimensional voxel-wise imaging phenotypes. We jointly incorporate the brain connectivity information and spatial correlation among voxels to enhance analytical power and biological interpretation.
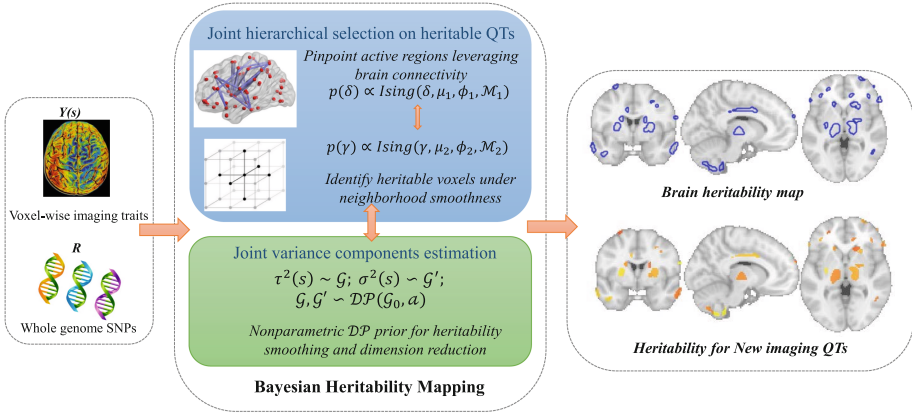
Fig. 1. The illustration of our proposed method Brain Heritability Mapping (BHM).

– We make the very first attempt to construct heritable imaging QTs with stronger genetic dissection power by removing the constrain from the traditional unsupervised brain atlas for the QT definition. These new QTs will provide a great potential to uncover in-depth genetic underpinnings.
– We demonstrate the effectiveness of our method in an empirical study to construct heritable imaging QTs using the structural magnetic resonance imaging (MRI) and genome-wide genotyping data from the ADNI cohort [12,15,20]. These novel imaging QTs are highly heritable in comparison with the heritable AAL-based QTs discovered by the standard GCTA method.

2   Method

Our overarching goal is to construct more powerful neuroimaging endophenotypes with strong genetic dissection power based on an innovative "brain heritability map". We propose a Bayesian semi-parametric model to jointly estimate voxel-specific heritability over whole brain imaging traits. Within the Bayesian paradigm, a hierarchical Ising-Spike-and-Slab prior is used to simultaneously impose sparsity on heritabilities at 1) brain regions while accounting for correlations induced by brain structural connectivity; 2) voxels while considering the dependency among adjacent voxels. To enhance biological insight and reduce parameter space, we further assign a Dirichlet process ($\mathcal{DP}$) prior on the genetic and environmental variance components, so that each of them are identical within a contiguous brain area. Based on the result, a brain heritability map can be constructed directly with the new imaging phenotype defined under the "active" subregions; and the heritability for each of them is also estimated. Please see Fig. 1 for the schematic design of our method.

Brain Heritability Mapping. To estimate the additive genetic heritability for imaging traits $\{y(s)\}_{s=1}^{S}$ over S voxels adjusting for clinical covariate $\mathbf{X}$, we

build the following mixed effect models

$$y(s) = \mathbf{X}\boldsymbol{\beta}(s) + g(s) + e(s), \quad s = 1, \ldots, S. \tag{1}$$

At each voxel s, $g(s)$ is the genetic random effect with $g(s) \sim \mathrm{N}(0, \mathbf{R}\tau^2(s))$, $\mathbf{R}$ is the empirical genetic relationship matrix among subjects that is calculated directly from the SNP data, and $\tau^2(s)$ is the variance explained by the genetics. The residual error $e(s) \sim \mathrm{N}(0, \mathbf{I}\sigma^2(s))$ with $\sigma^2(s)$ denotes the variance explained by the environmental effects. Based on the two variance components, the voxel-specific heritability can be calculated by $h(s) = \frac{\tau^2(s)}{\tau^2(s) + \sigma^2(s)}$ for $s = 1, \ldots, S$.

The assembly of $\{h(s)\}_{s=1}^S$ will provide a genetics cartographic map over the human brain. To impose a structural driven sparsity, we introduce a regional binary indicate set $\boldsymbol{\delta} = (\delta_1, \ldots, \delta_K)$ for the K ROIs and a voxel-level set $\boldsymbol{\gamma} = (\gamma_1, \ldots, \gamma_S)$ to jointly distinguish brain locations with and without active genetic impact. Based on them, we impose the following sparse group spike-and-slab prior for each genetic variance $\tau^2(s)$:

$$\tau^2(s) \sim (1 - \gamma(s)\delta(k))I_0 + \gamma(s)\delta(k)\mathcal{G}, \text{ with voxel } s \text{ belonging to region } k, \tag{2}$$

where I_0 is a point mass at zero, and $\mathcal{G}$ is a probability function where the nonzero component of $\tau^2(s)$ samples from. It is straightforward to see $\tau^2(s)$ (and $h(s)$) is nonzero only if $\gamma(s) = \delta(k) = 1$. Therefore, we can effectively narrow down heritable brain traits by stochastically excluding the regions with negligible genetic effect and only locate fine scale signals for the heritable regions.

To further induce a biologically plausible coupling of selection status in light of brain connectivity and spatial correlation, we resort to the Ising model for each of the indicator set

$$p(\boldsymbol{\delta}) \propto \mathrm{Ising}(\boldsymbol{\delta}, \mu_1, \phi_1, \mathcal{M}_1); \quad p(\boldsymbol{\gamma}) \propto \mathrm{Ising}(\boldsymbol{\gamma}, \mu_2, \phi_2, \mathcal{M}_2) \tag{3}$$

where graphs $\mathcal{M}_1$ and $\mathcal{M}_2$ summarize the region and voxel level structural information, and $\mu_1, \mu_2, \phi_1, \phi_2$ are the sparsity and smoothness parameters. Under hyper-prior (3), "connected" trait units have a higher possibility to be jointly included or excluded from the model, aligning with the biological expectation.

Imaging Endophenotype and Heritability Estimation. In terms of the environmental variance, we assume $\sigma^2(s) \sim \mathcal{G}'$ with a prior probability function $\mathcal{G}'$. Under such a fine scale voxel-level imaging phenotypes, it is biologically meaningful to assume the spatially contiguous voxels share similar heritability. To impose such smoothness of $\{h(s)\}$ over the identified contiguous hertiable brain areas, we assume the joint distribution of $\mathcal{G}$ and $\mathcal{G}'$ follows a nonparametric $\mathcal{DP}$ prior with scalar parameter α

$$\mathcal{G}, \mathcal{G}' \sim \mathcal{DP}(\mathcal{G}_0, \alpha), \quad \mathcal{G}_0 = \text{Inverse Gamma} \times \text{Inverse Gamma}', \tag{4}$$

where $\mathcal{G}_0$ is the base measure defined by a joint of two independent Inverse Gamma (IG) distributions. The nonparametric and discrete nature of (4) can

be clearly seen under the following sticking-breaking representation [13]

$$\mathcal{G} = \sum_{k=1}^{\infty} \pi_k I_{\theta_k}; \quad \mathcal{G}' = \sum_{k=1}^{\infty} \pi_k I_{\theta'_k}; \quad \theta_k, \theta'_k \sim \mathcal{G}_0; \qquad (5)$$

with $\pi_k = \pi'_k \prod_{h=1}^{k-1}(1 - \pi'_h)$ and $\pi'_k \sim \text{Beta}(1, \alpha)$. This allows us to more robustly accommodate the potential irregular distribution of variance components, while inducing a clustering effect of $\{h(s)\}$ with each contiguous area sharing the identical heritability estimate. Meanwhile, given the estimation unit of variance components moves from voxel to brain area, the risk of overfitting could be dramatically reduced with much less unknown parameters, and facilitate a more accurate heritability mapping estimation with meaningful smoothness effect.

Combing all the model specifications, we name our model Bayesian Heritability Mapping (BHM) which is semi-parametric; and develop a Markov chain Monte Carlo (MCMC) algorithm to conduct posterior inference. We rely on Gibbs samplers with data augmentation to obtain posterior draws embedded with a truncated stick-breaking process to approximate the $\mathcal{DP}$ representation. The eventual heritability map is captured by the median probability model [2] under the posterior inclusion probabilities of $\{\boldsymbol{\delta}\}$ and $\{\boldsymbol{\gamma}\}$. Simultaneously, we could obtain the heritability of each identified imaging QTs using the posterior median of $\{h(s)\}$. Given the defined QTs are the brain areas with active correspondence with genetics, we anticipate higher heritabilities of them than those under the traditional AAL defined regional imaging traits. Meanwhile, given the sparse nature of our method, we also expect a number of unwarranted regional heritable signals to be excluded from the result.

3   Experiments and Results

Data and Materials. The neuroimaging and genotypinig data used in this work were obtained from the Alzheimer's Disease Neuroimaging Initiative (ADNI) database (adni.loni.usc.edu) [12,15,20]. The up-to-date information about the ADNI is available at www.adni-info.org. The participants ($N = 1,472$) include 341 cognitively normal (CN), 85 significant memory concern (SMC), 265 early mild cognitive impairment (EMCI), 495 late MCI (LMCI), and 286 AD subjects at the ADNI-GO/2 baseline. See Table 1 for characteristics of these participants.

Structural MRI scans were processed with voxel-based morphometry (VBM) using the Statistical Parametric Mapping (SPM) software tool [1]. All scans were aligned to a T1-weighted template image, segmented into gray matter (GM), white matter (WM) and cerebrospinal fluid (CSF) maps, normalized to the standard Montreal Neurological Institute (MNI) space as $2 \times 2 \times 2\,\text{mm}^3$ voxels. The GM maps were extracted and smoothed with an 8mm FWHM kernel, and analyzed in this study. A total of 144,999 voxels, covering cortical, sub-cortical, and cerebellar regions and measuring GM density, were studied in this work as voxel-level imaging traits. Based on the AAL atlas [18], 116 ROI-level traits were also obtained by averaging all the voxel-level measures within each ROI.

Table 1. Participant characteristics. Age and sex are used as covariates in our study.

Diagnosis	CN	SMC	EMCI	LMCI	AD	Overall
Number	341	85	265	495	286	1472
Age (mean $\pm$ sd)	75.1 ± 5.4	72.4 ± 5.7	71.2 ± 7.1	73.9 ± 7.6	75.1 ± 8.0	73.9 ± 7.2
Sex (M/F)	182/159	36/49	147/118	306/189	162/124	833/639
Education(mean $\pm$ sd)	16.3 ± 2.6	16.7 ± 2.6	16.1 ± 2.6	16.0 ± 2.9	15.3 ± 3.0	16.0 ± 2.8
APOE $\epsilon 4$ present	24.9%	34.1%	36.2%	41.6%	46.5%	37.3%

For the genotyping data, we performed quality control using the following criteria: genotyping call rate >95 %, minor allele frequency >5%, and Hardy Weinberg Equilibrium >1e−6. A total of 565,373 SNPs were used for estimating heritability. The structural connectivity computed from diffusion MRI (dMRI) was used as connectivity information of the BHM model [8]. The preprocessed dMRI data of 291 participants were obtained from the human connectome project database, and the FSL software was used to construct the structural connectivity [21]. The distance-dependent consensus thresholding method was applied to generate group-level connectivity and to avoid overestimating short-range connections. This was used as the connectivity information in our analyses [3].

Implementation and Evaluation. We applied our proposed BHM model on the VBM and genetics data adjusting for age, sex and the first ten genetic principal components. The tuning parameters in the Ising priors were determined by the auxiliary method [11], the shape and scale parameters in the Inverse Gamma distributions were set to be 0.1 to provide non-informative support, and we assigned α to be a noninformative Gamma distribution $G(1, 1)$. We started with multiple chains with 10,000 iterations 5000 burn-in under random initials (`Matlab`2020b implementation, 2.4 GHz CPU, 64 GB Memory, Windows System). Each run took ∼6 h to finish, and both trace plots and GR method [7] were used to confirm the posterior convergence. We also implemented the GCTA model to calculate the marginal heritability of the AAL-based regional QTs using their provided pipeline in PLINK format. Eventually, we summarized the heritability for each ROI, our defined QT within the corresponding ROI, and the size in voxels of each heritable sub-region (Table 2).

ADNI Results. Table 2 shows the heritability estimation results of comparing the proposed BHM model and the traditional GCTA model, including 47 BHM-identified ROIs. For most of these ROIs, BHM was able to identify new imaging QTs (i.e., the subregion of each ROI with size indicated by $\mathbf{N_{Voxels}}$) with higher heritability than the GCTA-estimated heritability for the entire ROI based average measure. For instance, the BHM heritability estimates in bilateral superior frontal gyri (0.532, 0.409) are higher than GCTA results (0.124, 0.119). BHM also successfully captured working memory related regions better than GCTA, and these regions were known to be significantly heritable, including inferior, middle, and superior frontal gyri [4]. All these observations demonstrate the promise of the BHM method in identifying new highly heritable imaging QTs,

Table 2. Performance comparison. The GCTA column includes the heritability of the average VBM measure in the ROI estimated by the conventional GCTA method. The BHM column includes the BHM-estimated heritability of the identified imaging QT (i.e., the subregion of each ROI with size indicated by N_{Voxels}).

Region	Left hemisphere			Right hemisphere		
	GCTA	BHM	N_{Voxels}	GCTA	BHM	N_{Voxels}
Precentral				0.063	0.443	281
Frontal_Sup	0.124	0.532	352	0.119	0.409	429
Frontal_Sup_Orb	0.031	0.533	82	0.000	0.507	42
Frontal_Mid	0.109	0.321	331	0.003	0.446	259
Frontal_Inf_Oper	0.210	0.403	148	0.098	0.539	174
Frontal_Inf_Tri	0.014	0.390	194	0.223	0.452	564
Frontal_Inf_Orb				0.261	0.613	118
Rolandic_Oper				0.333	0.442	75
Frontal_Sup_Medial	0.311	0.323	264	0.265	0.421	227
Rectus	0.184	0.400	32	0.154	0.321	55
Cingulum_Ant				0.328	0.473	113
Cingulum_Mid	0.470	0.353	108			
Cingulum_Post				0.398	0.678	55
ParaHippocampal				0.240	0.487	41
Occipital_Inf				0.244	0.343	35
Postcentral	0.090	0.485	289	0.123	0.226	235
Parietal_Inf				0.336	0.554	66
SupraMarginal				0.172	0.428	62
Angular				0.028	0.391	56
Caudate	1.000	0.433	117	1.000	0.509	273
Putamen	0.000	0.288	312	0.000	0.377	356
Pallidum				0.068	0.419	75
Thalamus	0.720	0.445	446	0.613	0.391	324
Temporal_Pole_Sup	0.196	0.324	80	0.257	0.424	330
Temporal_Mid	0.091	0.340	123	0.085	0.478	298
Temporal_Pole_Mid	0.052	0.288	203	0.026	0.482	228
Temporal_Inf	0.000	0.323	101			
Cerebelum_8	0.322	0.450	409	0.456	0.369	150
Cerebelum_9	0.000	0.265	283	0.111	0.382	121
Cerebelum_10	0.285	0.132	58			

which can be used for subsequent in-depth brain imaging genetic analysis. Of note, some identified ROIs are relatively small and warrant replication in inde-
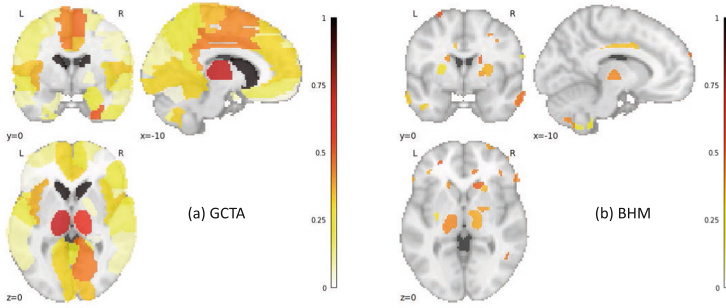
Fig. 2. Heritability maps estimated by (a) the conventional GCTA method and (b) the proposed BHM method. In the GCTA map, the entire ROI is painted with the estimated heritability. In the BHM map, only the identified voxels forming new heritable imaging QTs are painted with the estimated heritability.

Table 3. Simulation results under BHM, GCTA and MEGHA: RMSE for heritability estimation and AUC for heritability mapping. The Monte Carlo standard deviation is included in the parentheses.

Scenario	Method	IG(5, 10)		IG(0.5, 1)	
		RMSE	AUC	RMSE	AUC
$\mathcal{DP}$	GCTA	0.021 (6.211e−04)	0.966	0.043 (2.216e−05)	0.886
	MEGHA	0.013 (5.788e−05)	0.988	0.044 (6.824e−05)	0.960
	BHM	0.002 (3.578e−05)	0.999	0.002 (1.213e−04)	0.992
IG	GCTA	0.018 (3.431e−05)	0.914	0.032 (8.343e−05)	0.784
	MEGHA	0.005 (8.102e−06)	0.908	0.026 (3.877e−05)	0.792
	BHM	0.004 (8.354e−05)	0.995	0.004 (1.088e−04)	0.897

pendent cohorts. In addition, the GCTA method also identified some heritable traits that are worth detailed imaging genetic analysis.

Figure 2 shows the heritability maps estimated by (a) the conventional GCTA method and (b) the proposed BHM method. GCTA estimates the heritability of the average voxel measure of each ROI. Given that the AAL ROIs are quite large, the map looks nonsparse. However, the map covers part of the white matter region. This appears counter-intuitive, since VBM only measures gray matter density. In contrast, the BHM map identifies heritable voxels only in gray matter region, which appears to be biologically more precise and meaningful.

Simulation Results. We also perform simulations to evaluate the perform of BHM model compared with GCTA and massively expedited genome-wide heritability analysis (MEGHA) [5] in heritability mapping and estimation. We consider phenotypes measured over a 100×100 square with 10,000 voxels which is partitioned into 16 equally sized squared regions. Across the regions, we generate a scale-free connectivity network as prior information. We consider two scenarios

to generate environmental variance σ^2–Scenario 1 is to generate σ^2 based on a $\mathcal{DP}$ prior with base measure IG(0.5, 1), which fits our model assumption (see also Eq. (4)); Scenario 2 is to generate σ^2 directly from IG(0.5, 1). As for the genetic variance τ^2, we first set four pieces of significantly heritable areas lying over two regions including around 100 voxels, and then for the active signal index set $\mathcal{R}$, we generate $\tau^2(\mathcal{R}) \sim$ IG(5, 10) or $\tau^2(\mathcal{R}) \sim$ IG(0.5, 1) for two variance cases. For each of these simulated settings, we generate 100 MC datasets. The implementation of BHM and GCTA directly follows the ADNI study, and we use the publicly available pipeline for MEGHA with 10,000 permutation. We evaluate the heritability mapping performance by Area under Curve (AUC) for identifying the heritable voxels, and the heritability estimation by root-mean-square error (RMSE) for $h(s)$. All the results are summarized in Table 3.

In general, the proposed BHM model considerably outperforms GCTA and MEGHA in all the simulated settings for both heritability mapping and estimation. A higher variance in σ^2 expectedly deteriorates the model performance for all the methods. In addition, when the model assumption for BHM is not satisfied, we see minor decrease of AUC and increase of RMSE based on the proposed method, indicating the robustness of our approach.

4 Conclusion

We have proposed a new semi-parametric Bayesian heritability estimation model to construct highly heritable and biologically meaningful imaging quantitative traits (QTs). Our method leverages the aggregate of genetic signals to imaging QT construction by developing a new brain parcellation driven by voxel-level heritability. To ensure biological plausibility and clinical interpretablity of the resulting brain heritability parcellations, hierarchical sparsity and smoothness, coupled with structural connectivity of the brain, have been properly imposed on genetic effects to induce spatial contiguity of heritable imaging QTs. Using the ADNI imaging genetic data, we have demonstrated the strength of our proposed method, in comparison with the standard GCTA method, in identifying highly heritable and biologically meaningful new imaging QTs.

References

1. Ashburner, J., Friston, K.J.: Voxel-based morphometry-the methods. Neuroimage **11**(6), 805–21 (2000)
2. Barbieri, M.M., Berger, J.O., et al.: Optimal predictive model selection. Ann. Stat. **32**(3), 870–897 (2004)
3. Betzel, R.F., Griffa, A., Hagmann, P., Mišić, B.: Distance-dependent consensus thresholds for generating group-representative structural brain networks. Netw. Neurosci. **3**(2), 475–496 (2019)
4. Blokland, G.A., McMahon, K.L., Thompson, P.M., Martin, N.G., de Zubicaray, G.I., Wright, M.J.: Heritability of working memory brain activation. J. Neurosci. **31**(30), 10882–10890 (2011)

5. Ge, Y., et al.: Massively expedited genome-wide heritability analysis (megha). Proc. Natl. Acad. Sci. **112**(8), 2479–2484 (2015)
6. Ge, T., et al.: Multidimensional heritability analysis of neuroanatomical shape. Nat. Commun. **7**, e13291 (2016)
7. Gelman, A., Meng, X.L.: Simulating normalizing constants: from importance sampling to bridge sampling to path sampling. Stat. Sci. **13**, 163–185 (1998)
8. Glasser, M.F., et al.: The minimal preprocessing pipelines for the human connectome project. Neuroimage **80**, 105–124 (2013)
9. Hibar, D.P., et al.: Voxelwise gene-wide association study (vGeneWAS): multivariate gene-based association testing in 731 elderly subjects. Neuroimage **56**(4), 1875–91 (2011)
10. Luo, S., Song, R., Styner, M., Gilmore, J., Zhu, H.: FSEM: Functional structural equation models for twin functional data. J. Am. Stat. Assoc. **114**(525), 344–357 (2019)
11. Møller, J., Pettitt, A.N., Reeves, R., Berthelsen, K.K.: An efficient Markov chain Monte Carlo method for distributions with intractable normalising constants. Biometrika **93**(2), 451–458 (2006)
12. Saykin, A.J., et al.: Genetic studies of quantitative MCI and AD phenotypes in ADNI: progress, opportunities, and plans. Alzheimers Dement. **11**(7), 792–814 (2015)
13. Sethuraman, J.: A constructive definition of dirichlet priors. Stat. Sin. **4**, 639–650 (1994)
14. Shen, L., Thompson, P.M.: Brain imaging genomics: integrated analysis and machine learning. Proc. IEEE Inst. Electr. Electron. Eng. **108**(1), 125–162 (2020)
15. Shen, L., et al.: Genetic analysis of quantitative phenotypes in AD and MCI: imaging, cognition and biomarkers. Brain Imaging Behav. **8**(2), 183–207 (2014)
16. Stein, J.L., et al.: Voxelwise genome-wide association study (vGWAS). Neuroimage **53**(3), 1160–74 (2010)
17. Thompson, P.M., et al.: Genetic influences on brain structure. Nat. Neurosci. **4**(12), 1253–8 (2001)
18. Tzourio-Mazoyer, N., et al.: Automated anatomical labeling of activations in SPM using a macroscopic anatomical parcellation of the MNI MRI single-subject brain. Neuroimage **15**(1), 273–89 (2002)
19. Visscher, P.M., Hill, W.G., Wray, N.R.: Heritability in the genomics era-concepts and misconceptions. Nat. Rev. Genet. **9**(4), 255–66 (2008)
20. Weiner, M.W., et al.: Recent publications from the Alzheimer's disease neuroimaging initiative: reviewing progress toward improved ad clinical trials. Alzheimer's Dementia **13**(4), e1–e85 (2017)
21. Woolrich, M.W., et al.: Bayesian analysis of neuroimaging data in FSL. Neuroimage **45**(1), S173–S186 (2009)
22. Yang, J., Lee, S.H., Goddard, M.E., Visscher, P.M.: GCTA: a tool for genome-wide complex trait analysis. Am. J. Hum. Genet. **88**(1), 76–82 (2011)
23. Yao, X., et al.: Mining regional imaging genetic associations via voxel-wise enrichment analysis. In: 2019 IEEE EMBS International Conference on Biomedical & Health Informatics (BHI), pp. 1–4 (2019)
24. Zhao, B., et al.: Heritability of regional brain volumes in large-scale neuroimaging and genetic studies. Cereb. Cortex **29**(7), 2904–2914 (2019)
25. Zhao, Y., Li, T., Zhu, H.: Bayesian sparse heritability analysis with high-dimensional neuroimaging phenotypes. Biostatistics, kxaa035 (2020). https://doi.org/10.1093/biostatistics/kxaa035